Title

Evaluating the Efficacy of Combination CD46-Targeted 225Ac Radioimmunotherapy and Antibody-Drug Conjugate Therapy in Multiple Myeloma

Author

Mayne, Ellis

Publication Date

2024

Peer reviewed|Thesis/dissertation

Evaluating the Efficacy of Combination CD46-Targeted 225Ac Radioimmunotherapy and Antibody-Drug Conjugate Therapy in Multiple Myeloma

by

Ellis Mayne

THESIS

Submitted in partial satisfaction of the requirements for degree of

MASTER OF SCIENCE

in

Biomedical Imaging

in the

GRADUATE DIVISION

of the

UNIVERSITY OF CALIFORNIA, SAN FRANCISCO

Approved:

DocuSigned by:
Robert Flavell
DE54D221721B45E...

Robert Flavell

Chair

DocuSigned by:
Henry Vanbrocklin
[illegible]4B1...

Henry Vanbrocklin

DocuSigned by:
Youngho Seo
[illegible]484...

Youngho Seo

DocuSigned by:
Michael Evans
40E92A530F764EE...

Michael Evans

Committee Members

Acknowledgements

I want to thank my advisor, Robert Flavell, MD, PhD, and committee members Henry VanBrocklin, PhD, Youngho Seo, PhD, and Michael Evans, PhD for their feedback and support throughout my research and thesis-writing experience at UCSF. I would also like to thank all members of the Flavell Lab for welcoming me into the fold and for sharing their knowledge with me. I am especially grateful for the guidance of my postdoctoral mentor Anju Wadhwa, PhD, who dedicated so much time to teaching me the radiochemistry, biology, and image analysis skills required to accomplish this work. Additionally, I would like to acknowledge Bin Liu, PhD and Scott Bidlingmaier, PhD for their help with this work, especially for their effort in producing the YS5 antibody and CD46 antibody-drug conjugate that were used in our experiments. Finally, I would like to thank my family and friends for their encouragement over the past year.

Evaluating the Efficacy of Combination CD46-Targeted ^{225}Ac Radioimmunotherapy and Antibody-Drug Conjugate Therapy in Multiple Myeloma

Ellis Mayne

Abstract

Multiple myeloma is one of the most common blood cancers. Many drugs have been developed to treat multiple myeloma, yet refractory and relapsed disease remain prevalent. The recent identification of CD46, an antigen overexpressed on multiple myeloma cells, has led to new development of antibody-based immunotherapies, including the antibody-drug conjugate CD46 ADC and the radioimmunotherapy [^{225}Ac]Ac-Macropa-PEG$_4$-YS5. The structures of both drugs include the CD46-binding monoclonal antibody YS5, and both have shown high tumor binding and antitumor efficacy in pre-clinical models for multiple myeloma. A Phase 1 clinical trial is also underway to evaluate CD46 ADC in multiple myeloma. While initial results are promising, both drugs have noted drawbacks, with blood cancers like multiple myeloma known to develop resistance to ADCs over time and [^{225}Ac]Ac-Macropa-PEG$_4$-YS5 studies displaying nephrotoxicity at higher doses. Hypothesizing that the use of the two drugs in tandem could improve therapeutic efficacy, this study investigated the performance of RIT & ADC combined treatment across preclinical multiple myeloma models *in-vitro* and *in-vivo*. Results of initial cell-based assays demonstrated a high cell killing ability of combination treatment, with evidence of a synergistic interaction between drugs at select combination concentrations. A pilot xenograft mouse model comparing combination treatment to RIT & ADC monotherapies showed a widespread reduction in tumor burden with animal body weight remaining stable, potentially indicating reduced off-target toxicity. Future work will monitor the antitumor efficacy of RIT &

ADC combination therapy over a longer time scale and measure organ damage *ex-vivo* to further compare against prior monotherapy results. This encouraging initial data provides guidance on combination dosing regimens for future preclinical research and suggests that RIT & ADC combination therapy may be a valuable clinical option for treating multiple myeloma.

Table of Contents

List of Figures

List of Abbreviations

^{225}Ac – Actinium-225

ITLC – Instant Thin Layer Chromatography

MMAE – Monomethyl Auristatin E

MMAF – Monomethyl Auristatin F

RIT – Radioimmunotherapy

ADC – Antibody-Drug Conjugate

M – moles per liter

BLI – Bioluminescence Imaging

IC_{50} – Half-Maximal Inhibitory Concentration

ROI – Region of Interest

FBS – Fetal Bovine Serum

1 Introduction

Multiple myeloma is one of the most prevalent hematological malignancies, making up 19% of new blood cancer cases diagnosed in the United States in 2023.[1] The disease is characterized by a proliferation of cancerous plasma cells in the bone marrow. The buildup of these myeloma cells leads to the production of monoclonal proteins and a reduction of healthy white blood cells, red blood cells, and platelets. Resulting symptoms include a weakened immune system, anemia, bone destruction, kidney failure, and more.

Years of research in multiple myeloma have brought numerous therapies into the clinic. Patients commonly receive multi-drug treatments that can include a monoclonal antibody, an immunomodulatory agent (IMiD), a proteasome inhibitor, and/or a steroid.[2] Eligible patients may then be given an autologous stem cell transplant (ASCT) designed to resume healthy blood cell production in the bone marrow. Additional novel immunotherapies designed to direct the immune system's killer T-cells towards myeloma cells have seen recent FDA approvals for use in refractory or relapsed multiple myeloma cases. These drugs include CAR-T therapies idecabtagene vicleucel and ciltacabtagene autoleucel and bispecific antibodies teclistamab-cqyv and elranatamab-bcmm.[3] While patient outcomes for multiple myeloma have improved, the disease eventually becomes refractory to many of these drugs and relapse is common. Therefore, additional drug targets and novel therapy options for patients are needed.

Recent work by researchers at UCSF, led by Bin Liu, PhD, have identified the antigen CD46 as a target for multiple myeloma. CD46 is located on chromosome 1q, which is commonly overexpressed on multiple myeloma cells and becomes more amplified at relapse.[4] CD46 is also overexpressed on other cancers including prostate, ovarian cancer, breast cancer, and leukemia.

Employing a novel method of phage antibody library selection utilizing laser capture microdissection, the Liu Lab discovered a human monoclonal antibody YS5 that targets CD46 with a high tumor to background ratio. After binding with CD46, YS5 is internalized by macropinocytosis.[4] These discoveries have unlocked new potential for targeted therapy options for refractory or relapsed multiple myeloma.

The first CD46 targeted therapy to be developed was the antibody-drug conjugate CD46 ADC. It consists of the YS5 antibody conjugated to a monomethyl auristatin E (MMAE) or a monomethyl auristatin F (MMAF) cell-killing toxic payload.[4] Both MMAE and MMAF are commonly used payloads for approved antibody-drug conjugates. ADCs perform best when the cytotoxic payload is released into the cell, emphasizing the importance of YS5's internalization via macropinocytosis. Across *in-vitro* and *in-vivo* studies of multiple myeloma, CD46 ADC has demonstrated high tumor-selective binding and high antitumor efficacy. Furthermore, multi-center Phase 1 clinical trials to evaluate the therapeutic efficacy of CD46 ADC for both multiple myeloma (NCT03650491) and prostate cancer patients (NCT03575819) are ongoing.[5] The chemical structure of CD46 ADC is shown in **Figure 1.**

More recently, the Flavell Lab has used YS5 to investigate a novel radioimmunotherapy agent [^{225}Ac]Ac-DOTA-YS5. Utilizing the radioisotope actinium-225, [^{225}Ac]Ac-DOTA-YS5 releases four high energy alpha-particles in its decay chain over a tissue distance of 50-100 μm.[6] This delivers a powerful treatment to the CD46-expressing target that can result in double DNA strand breaks while minimizing harmful energy transfer to the surrounding healthy tissue.[6] Like CD46 ADC, [^{225}Ac]Ac-DOTA-YS5 has shown promising antitumor efficacy in pre-clinical multiple myeloma models.[5] A schematic displaying the treatment pathway of [^{225}Ac]Ac-DOTA-YS5 can be viewed in **Figure 2** and its chemical structure is seen in **Figure 3.** As part of the same

work, a positron-emitting theranostic matched pair for [^{225}Ac]Ac-DOTA-YS5 has been developed for PET imaging. With this immunoPET probe [^{89}Zr]Zr-DFO-YS5, CD46-expressing multiple myeloma cells can be visualized prior to treatment with [^{225}Ac]Ac-DOTA-YS5.[7]

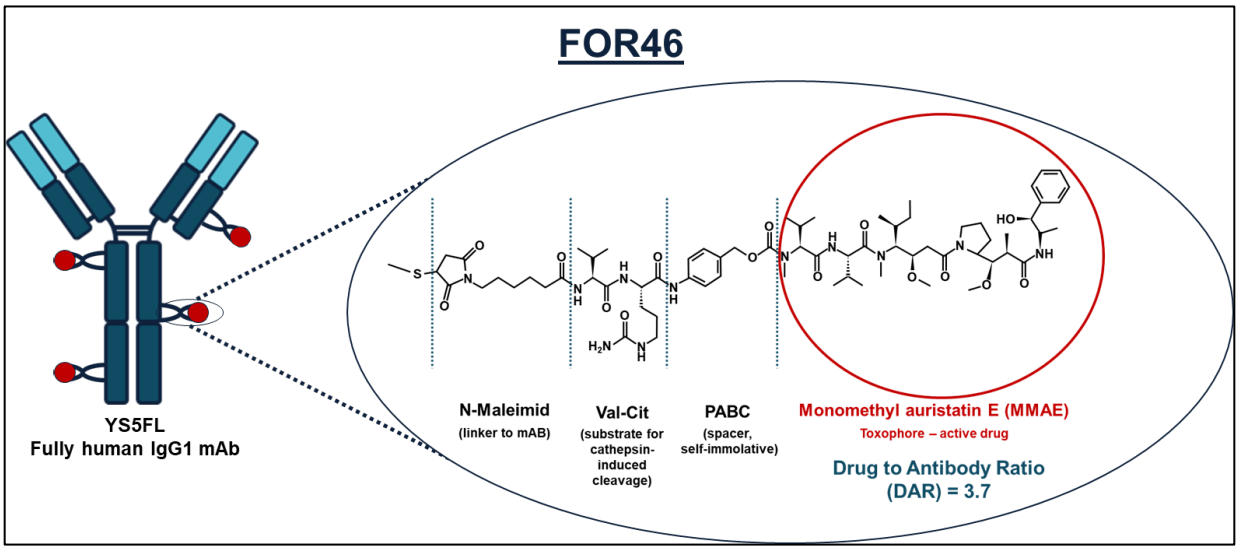

Figure 1: Chemical structure of CD46 ADC, developed by the Liu Lab, UCSF.[8]

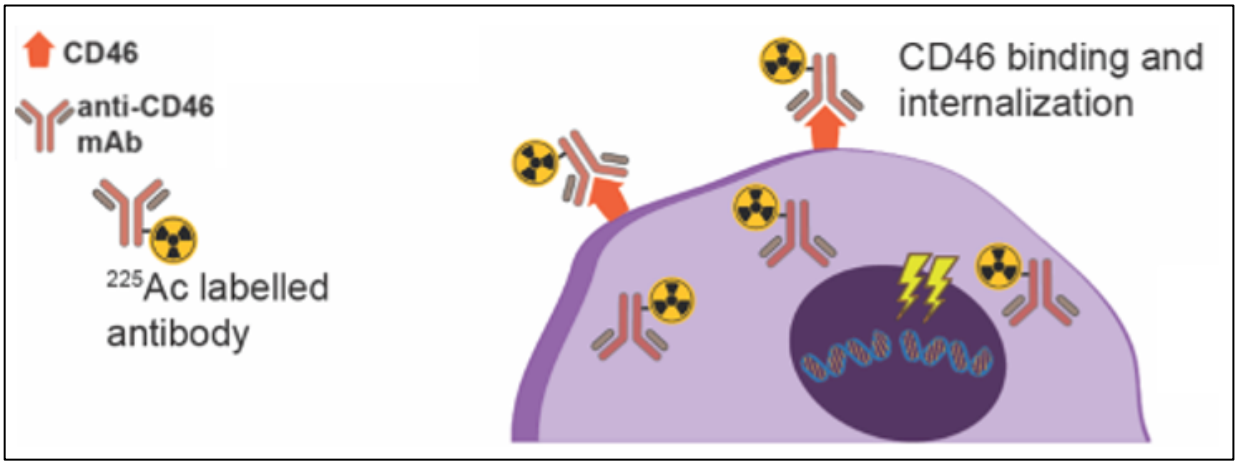

Figure 2: Schematic demonstrating the binding of an ^{225}Ac labeled YS5 antibody (anti-CD46 mAb) with the CD46 antigen on the cancer cell surface.[9] After binding, the radioligand is internalized. CD46 ADC is similarly internalized following binding with CD46.

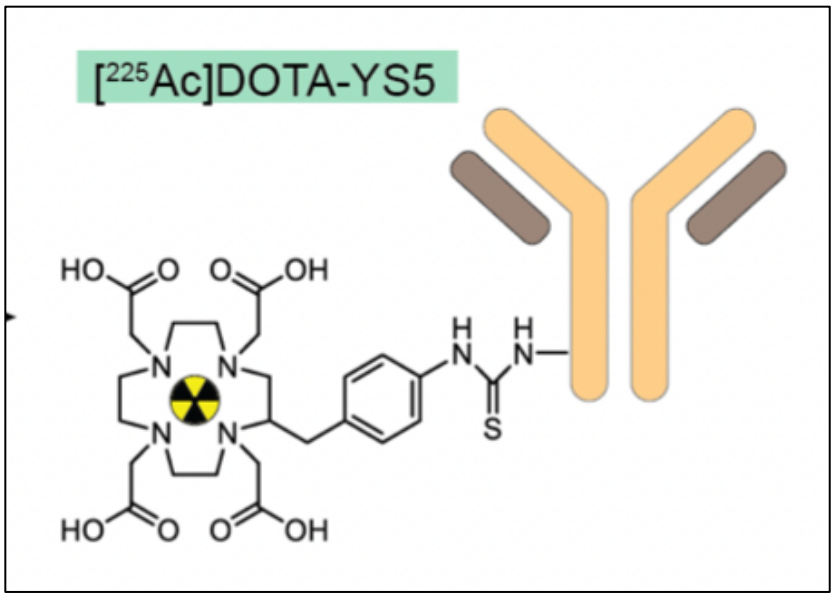

Figure 3: Chemical structure of [^{225}Ac]Ac-DOTA-YS5, a CD46-targeted radioimmunoconjugate that has been evaluated as a monotherapy in pre-clinical models by the Flavell Lab.[7]

Both CD46 ADC and [^{225}Ac]Ac-DOTA-YS5 RIT have shown significant promise in treating multiple myeloma in pre-clinical models, yet there are noted limitations to both treatments. Patients treated with antibody-drug conjugates such as CD46 ADC commonly experience disease progression over time, developing resistance that ultimately reduces the effectiveness of the therapy.[10] In [^{225}Ac]Ac-DOTA-YS5 therapy studies performed in xenograft mouse models for multiple myeloma and prostate cancer, nephrotoxicity has been observed at high doses. Data supports that this damage occurs when ^{225}Ac daughter isotopes ^{213}Bi and ^{221}Fr are ejected from the chelator due to the nuclear recoil effect, resulting in harmful isotope accumulation in the kidneys.[7] Recent work has shown that using the chelator and linker pair Macropa-PEG$_4$ in place of DOTA may help reduce some off-target toxicity, but kidney damage remains a significant side effect of ^{225}Ac-based RITs.[11] Therefore, while there is considerable potential for clinical translation for both CD46 ADC and [^{225}Ac]Ac-Macropa-PEG$_4$-YS5 therapies, additional efforts must be made to further improve efficacy and minimize side effects of the treatments.

Until now, combination treatment of CD46 ADC and [^{225}Ac]Ac-Macropa-PEG$_4$-YS5 had not been explored. This thesis project seeks to evaluate the efficacy of CD46-targeted RIT & ADC combination therapy via a series of *in-vitro* and *in-vivo* multiple myeloma models. These preclinical experiments measured key therapeutic factors such as cell-killing, reduction in tumor burden, survival, and organ toxicity, designed to establish an optimized dosing regimen for future combination therapy studies. This work is intended to supplement prior mono-therapeutic research in CD46-targeted RIT & ADC therapies with the goal of improving and expanding clinical treatment options for multiple myeloma.

2 Methods

2.1 Antibody Conjugation and Radiolabeling of [^{225}Ac]Ac-Macropa-PEG$_4$-YS5

All experiments required the conjugation of the YS5 antibody with chelator Macropa, followed by radiolabeling with ^{225}Ac. In the Flavell Lab's prior work evaluating the mono-therapeutic [^{225}Ac]Ac-DOTA-YS5 in a disseminated model of multiple myeloma, the chelator DOTA was used. In this study, Macropa was used in place of DOTA due to its enhanced radiolabeling kinetics, as demonstrated in a recent study.[11] A PEG$_4$ linker was also used in the conjugation as it has demonstrated a higher tumor-to-organ ratio and faster blood clearance *in-vivo*, reducing off-target toxicity.[11]

Conjugation of YS5 with Macropa-PEG$_4$-TFP ester was previously optimized by members of the Flavell Lab[11] and the protocol was followed for this work. Using a YM30K MW centrifugal filter unit (Millipore), 1 mg of YS5 was filtered three times with 400 µL of 0.1 M Na_2CO_3-$NaHCO_3$ buffer (pH 9.0) and then adjusted to a final concentration of 5 mg/mL. 1 mg of Macropa-

PEG_4-TFP ester was dissolved in 50 μL of DMSO. YS5 was combined with 7.5 equivalents of Macropa-PEG_4-TFP ester in DMSO and incubated at 37°C for 2 hours. A PD10 gel column (GE Healthcare) was then used to purify the resulting conjugation by elution of 0.25 M NaOAc (pH = 6).

Radiolabeling of Macropa-PEG_4-YS5 with ^{225}Ac was performed by combining 25 μCi of ^{225}Ac (10 μL) with 50 μL of 2M NH_4OAc (pH 5.8), 20 μL of L-Ascorbic acid (150 mg/mL), and 4 μL of Macropa-PEG_4-YS5 (25.13 mg/mL) and incubating the resulting solution at 37°C for 30 minutes. Instant thin layer chromatography (ITLC) was performed immediately following incubation by placing a small sample on silica gel chromatography paper and eluting with 10 mM EDTA (pH 5.5). Filtration via centrifuge was then performed on the radiolabeled sample using a YM30K filtration unit, with 400 μL of 0.9% saline passed through the unit three times. Following filtration, ITLC was again performed to confirm radiochemical purity.

CD46 ADC was sourced directly from UCSF collaborators and featured the conjugation of the MMAE toxic payload to the YS5 antibody with a lysosomal protease–sensitive valine-citrulline linker.[4]

2.2 In-*Vitro* Assays

Cell Culture

Multiple myeloma cell line MM.1s was utilized in each of the performed combination studies. These cells were grown suspended in RPMI1640 medium including 10% FBS, 100 U penicillin, and 100 μg/mL streptomycin and kept in a humidified incubator at 37°C and 5% CO_2. All MM.1s cells were engineered to express luciferase, enabling bioluminescence imaging

techniques used *in-vitro* and *in-vivo.* All cells were monitored for contamination prior to use in all experiments.

Cell Viability Assays

Cell viability assays were performed and optimized *in-vitro* to evaluate the cell-killing of CD46 ADC and [^{225}Ac]Ac-Macropa-PEG$_4$-YS5 RIT at combination doses of varying concentration. These studies were run in 96 well plates containing 2000 MM.1s cells/well. Each concentration of CD46 ADC and [^{225}Ac]Ac-Macropa-PEG$_4$-YS5 RIT was tested in triplicate across plates, including wells treated solely with CD46 ADC or [^{225}Ac]Ac-Macropa-PEG$_4$-YS5 RIT monotherapy concentrations. Cells were counted 96 hours after treatment via luminescence using CellTiter-Glo (Promega Corporation). Viability and inhibition plots were generated by comparing cell counts to averaged untreated media control.

Assessing RIT & ADC Combination Treatment Synergy

The therapeutic effects of combination therapy were further evaluated via zero interaction potency (ZIP) analysis. With this model, dose response curves of combination CD46 ADC and [^{225}Ac]Ac-Macropa-PEG$_4$-YS5 RIT treatment were compared to each drug's respective monotherapy curves across all dose concentrations. Synergistic potency scores were calculated for each combination RIT & ADC concentration.

2.3 *In-Vivo* Combination Therapy

Animal Model

RIT & ADC combination therapy was evaluated *in-vivo* in a disseminated xenograft mouse model. The University of California, San Francisco Institutional Animal Care and Use Committee (UCSF-IACUC) approved the use of 20 immunodeficient NSG mice (Jackson Laboratories) for this pilot study.

Experiment Design

All 20 mice were inoculated with 0.5 million MM.1s cells intravenously to establish the disseminated model. Seven days after inoculation, the mice were split into four groups, with each group initially containing n = 5 animals. Varying doses of [^{225}Ac]Ac-Macropa-PEG$_4$-YS5 and CD46 ADC were studied across each group. The first group of mice was considered a vehicle and injected with saline, the second group was injected with a 1.8 mg/kg dose of CD46 ADC, the third group was injected with a 0.0625 μCi dose of [^{225}Ac]Ac-Macropa-PEG$_4$-YS5, and the fourth group was injected with a combination dose of 1.8 mg/kg dose of CD46 ADC and 0.0625 μCi of [^{225}Ac]Ac-Macropa-PEG$_4$-YS5. All mice were also injected with 0.5 mg of IgG antibody at the time of treatment to block the Fc receptor, reducing non-specific binding of YS5.[12] A detailed diagram of the *in-vivo* protocol is included in **Figure 4**.

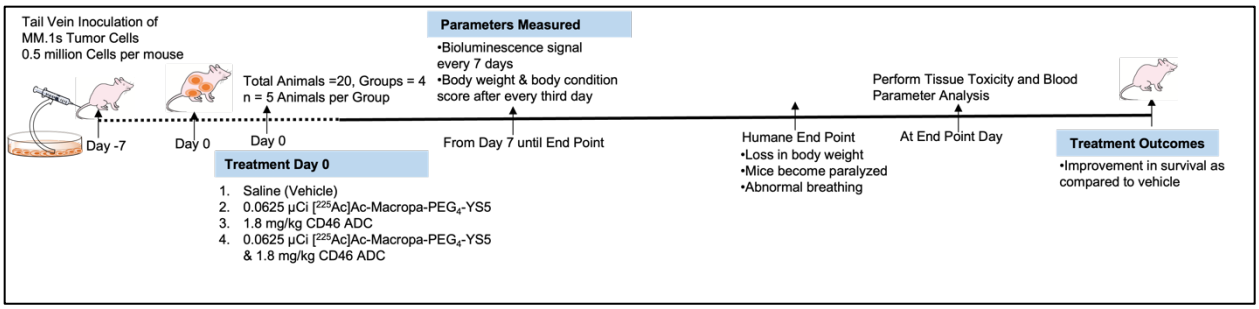

Figure 4: Diagram summarizing the protocol for the RIT & ADC combination therapy pilot study in a disseminated xenograft mouse model.

Experimental Data Collection

Body weights were recorded twice per week, with mice reaching their ethical endpoints if more than 20% weight loss was observed. Bioluminescence imaging was performed on an IVIS optical imaging system once per week to monitor tumor burden in each group. Regions of interest were drawn on BLI images to quantify tumor burden per mouse and compare across treatment groups. Overall mouse survival was measured with a Kaplan-Meier plot.

At the time of writing, this study is still ongoing. After the endpoint day (expected to be Day 120) is reached, remaining mice will be imaged with an immunoPET probe to supplement tumor burden data generated from bioluminescence imaging. Furthermore, blood samples and organs will be collected from surviving mice and analyzed for toxicity by collaborators at University of California, Davis.

3 Results

3.1 Antibody Conjugation and Radiolabeling of [^{225}Ac]Ac-Macropa-PEG$_4$-YS5

The radiosynthesis of [^{225}Ac]Ac-Macropa-PEG$_4$-YS5 was performed successfully, with the resulting chemical structures following conjugation and radiolabeling steps shown in the diagram in **Figure 5**. ITLC analysis performed immediately after synthesis is displayed in **Figure 6**, demonstrating a radiochemical purity of nearly 93% prior to filtration. The radiosynthesis process was repeated several more times over the course of all experiments, with crude radiochemical purity maintaining a value of at least 91%.

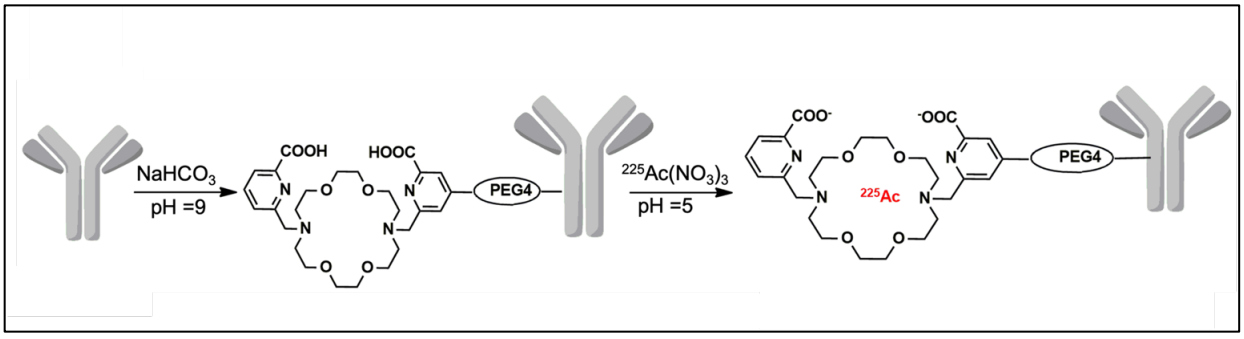

Figure 5: Synthesis diagram of [^{225}Ac]Ac-Macropa-PEG$_4$-YS5, beginning with conjugation of YS5 antibody with Macropa-PEG$_4$-TFP ester followed by radiolabeling with ^{225}Ac.

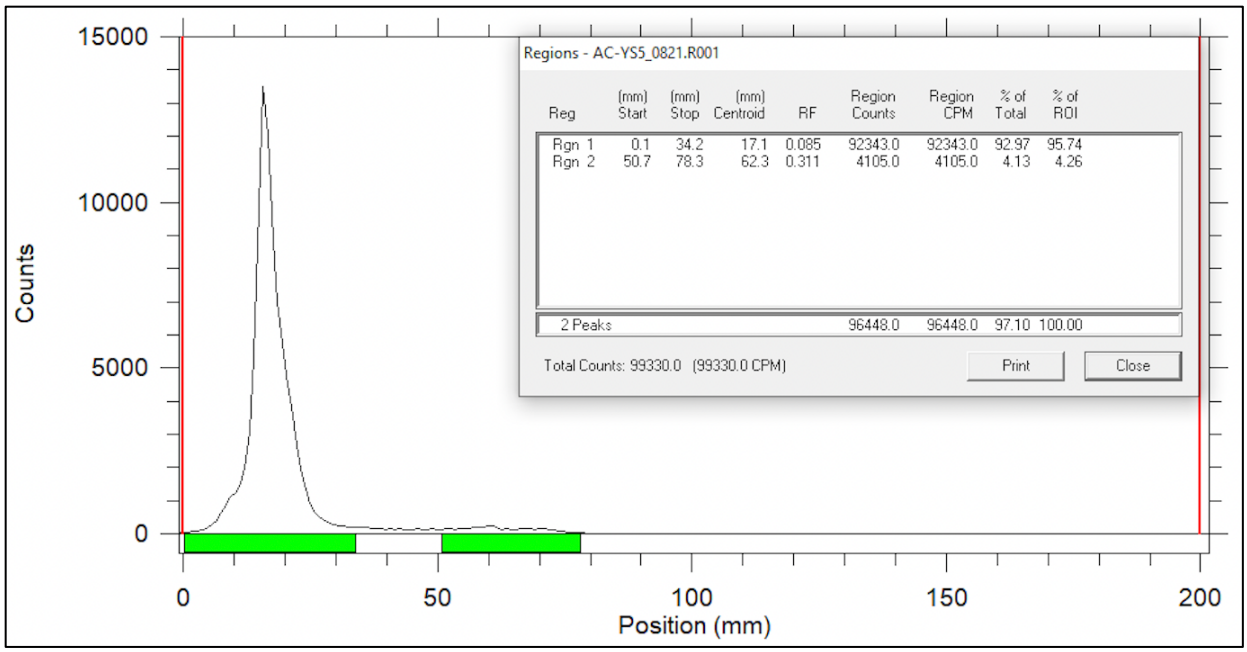

Figure 6: ITLC results of [^{225}Ac]Ac-Macropa-PEG$_4$-YS5 synthesis measured immediately after incubation. Results demonstrate approximately 93% radiochemical purity of [^{225}Ac]Ac-Macropa-PEG$_4$-YS5.

3.2 *In-Vitro* Assays

Cell Viability Assay

Prior to running cell viability assays for combination RIT & ADC therapy, initial monotherapy assays were run to optimize dose concentration ranges and establish IC$_{50}$ values. The cell viability results of CD46 ADC monotherapy can be found in **Figure 7.** Tested concentrations ranged from 150 nM to 0.146 nM. The IC$_{50}$ value was found to be 0.370 nM, indicating the dose required to achieve a 50% live cell count compared to control. **Figure 8** displays cell viability results of [^{225}Ac]Ac-Macropa-PEG$_4$-YS5 RIT monotherapy. Concentrations ranged from 500 nCi/mL to 0.0977 nCi/mL. IC$_{50}$ was found to be 0.187 nCi/mL.

Results of the combination RIT & ADC therapy cell viability assay are depicted as a matrix in **Figure 9.** Tested concentrations ranged from 0.8 nM to 0.025 nM for CD46 ADC and 0.6 nCi/mL to 0.00469 nCi/mL for [^{225}Ac]Ac-Macropa-PEG$_4$-YS5. Results are depicted as percent inhibition, describing the percentage of cells *killed* compared to control wells. RIT & ADC monotherapy concentrations in this combination assay generated similar results to **Figure 7** & **Figure 8,** with IC_{50} calculated as 1.26 nM for CD46 ADC and 0.42 nCi/mL for [^{225}Ac]Ac-Macropa-PEG$_4$-YS5.

Results of ZIP analysis of the combination cell viability assay are also shown in **Figure 9**. The highest synergistic interaction between RIT & ADC therapies was found approximately between ADC concentrations of 0.4 and 0.1 nM and RIT concentrations of 0.6 and 0.15 nCi/mL.

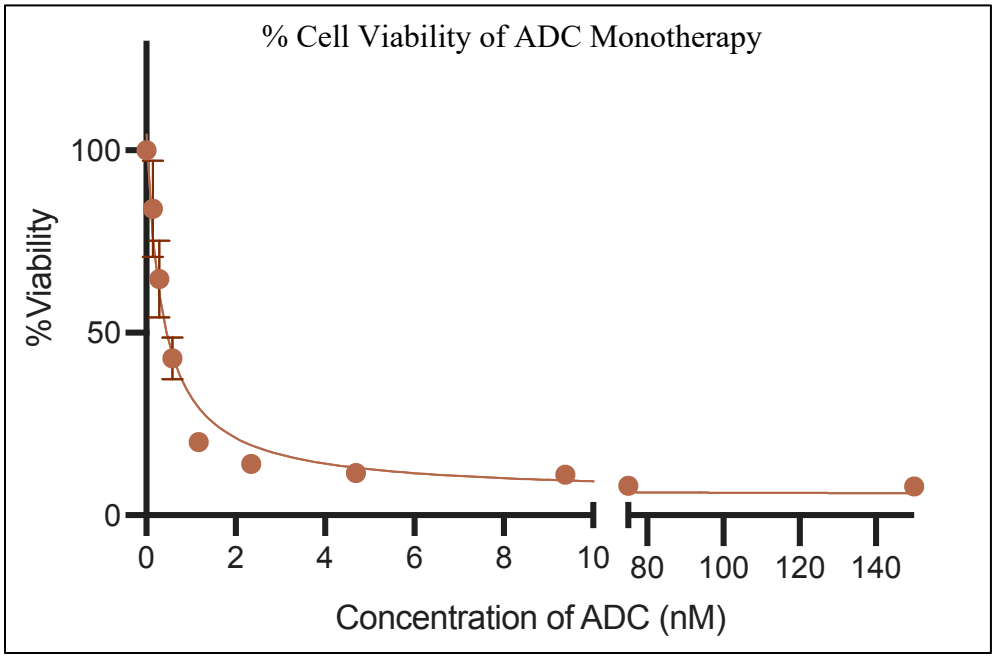

Figure 7: Cell viability results of wells treated with CD46 ADC monotherapy. Tested concentrations ranged from 150 nM to 0.146 nM. An IC_{50} value of 0.37 nM was derived from an interpolated curve produced in GraphPad Prism software.

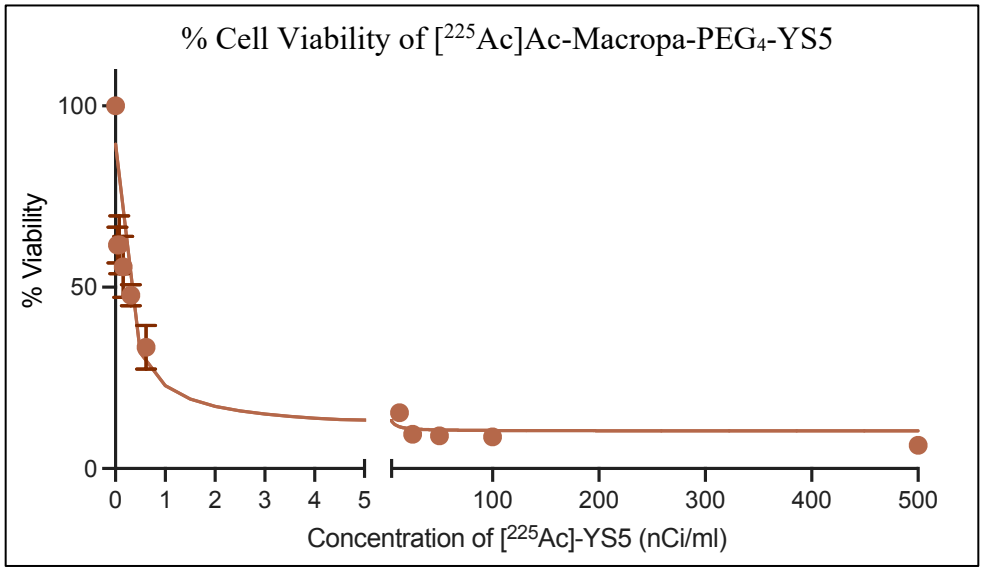

Figure 8: Cell viability results of wells treated with [^{225}Ac]Ac-Macropa-PEG$_4$-YS5 monotherapy. Tested concentrations ranged from 500 nCi/mL to 0.0977 nCi/mL. An IC_{50} value of 0.187 nCi/mL was derived from an interpolated curve produced in GraphPad Prism software.

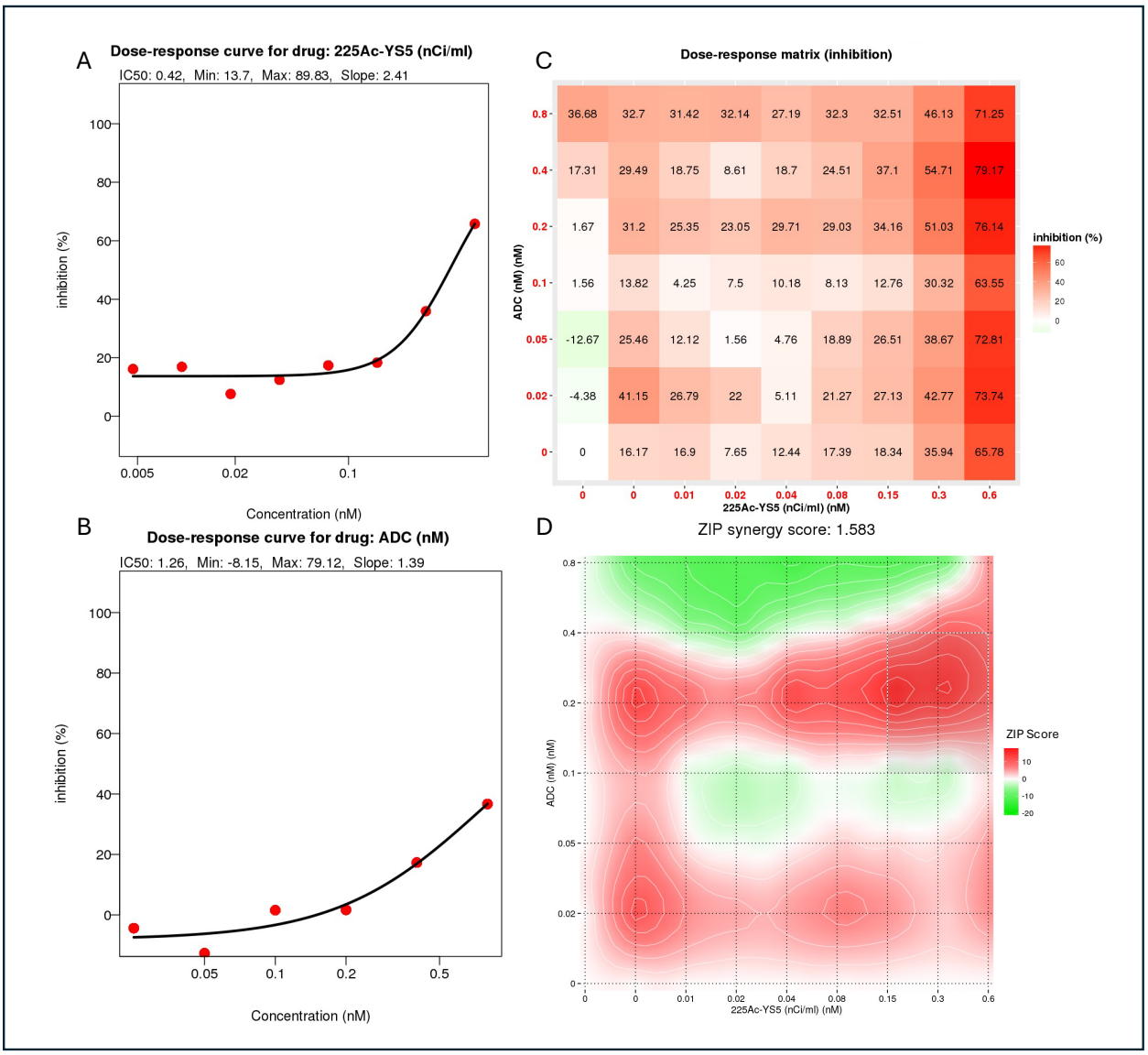

Figure 9: (A) Dose-response curve of [^{225}Ac]Ac-Macropa-PEG$_4$-YS5 monotherapy measured in the combination cell viability assay. **(B)** Dose-response curve of CD46 ADC monotherapy measured in the combination cell viability assay. **(C)** Dose-response matrix describing cell inhibition percentage at varying concentrations of RIT & ADC combination therapy, including monotherapies. The smallest evaluated RIT concentration, 0.00469 nCi/mL, is noted as 0 nCi/mL at the second to left-most column. **(D)** Synergy scores are displayed for each dose concentration of RIT & ADC, with a positive value representing a synergistic drug interaction, a near-zero value representing an additive interaction, and a negative value representing an antagonistic dose relationship. The average synergy score across all combination concentrations is displayed above the figure. All plots were produced with SynergyFinder software.

3.3 *In-Vivo* Combination Therapy

At the time of writing, data was obtained through the first 42 days of RIT & ADC therapy in the MM.1s disseminated xenograft mouse model. Weekly bioluminescence imaging data can be found in **Figure 10.** At the beginning of the experiment, one of the five mice in the RIT group died due to complications from MM.1s cell inoculation. At Day 0, seven days after inoculation, all groups displayed some level of signal, indicating the presence of tumor burden. At Day 14, the saline group displayed an increased level of signal, while the three treatment groups showed a decrease in tumor burden. By Day 28, the saline group had seen tumor burden continue to rise and the ADC group showed the presence of tumor in three mice, while the RIT group and RIT & ADC combination group maintained a very low level of signal. At Day 42, only two saline mice remained, while high signal was seen in four ADC monotherapy mice. Three RIT monotherapy mice had begun to show recurrent disease and one mouse from the RIT & ADC group displayed tumor burden.

Further assessing differences in tumor burden across treatment groups via BLI, **Figure 11** displays quantitative signal intensities obtained from drawn ROIs. All treatment groups showed lower average radiance compared to the saline group through Day 42. ADC monotherapy showed the highest average radiance among treatment groups, with combination RIT & ADC therapy showing slightly higher average radiance than RIT monotherapy largely due to disease seen in a single mouse. Average radiance in the saline group fell between Day 35 and 42 after three mice with significant tumor burden were euthanized.

Results from body weight monitoring through Day 42 can be found in **Figure 12.** Through Day 42, average body weights of mice across all treatment groups remained higher than average

weights measured at the start of treatment. After a period of decline, average body weight of the saline group grew at Day 42 following the loss of three mice.

Figure 13 displays overall mouse survival through Day 42 of the study via a Kaplan-Meier plot. Since the therapy began on Day 0, no treated mice have died.

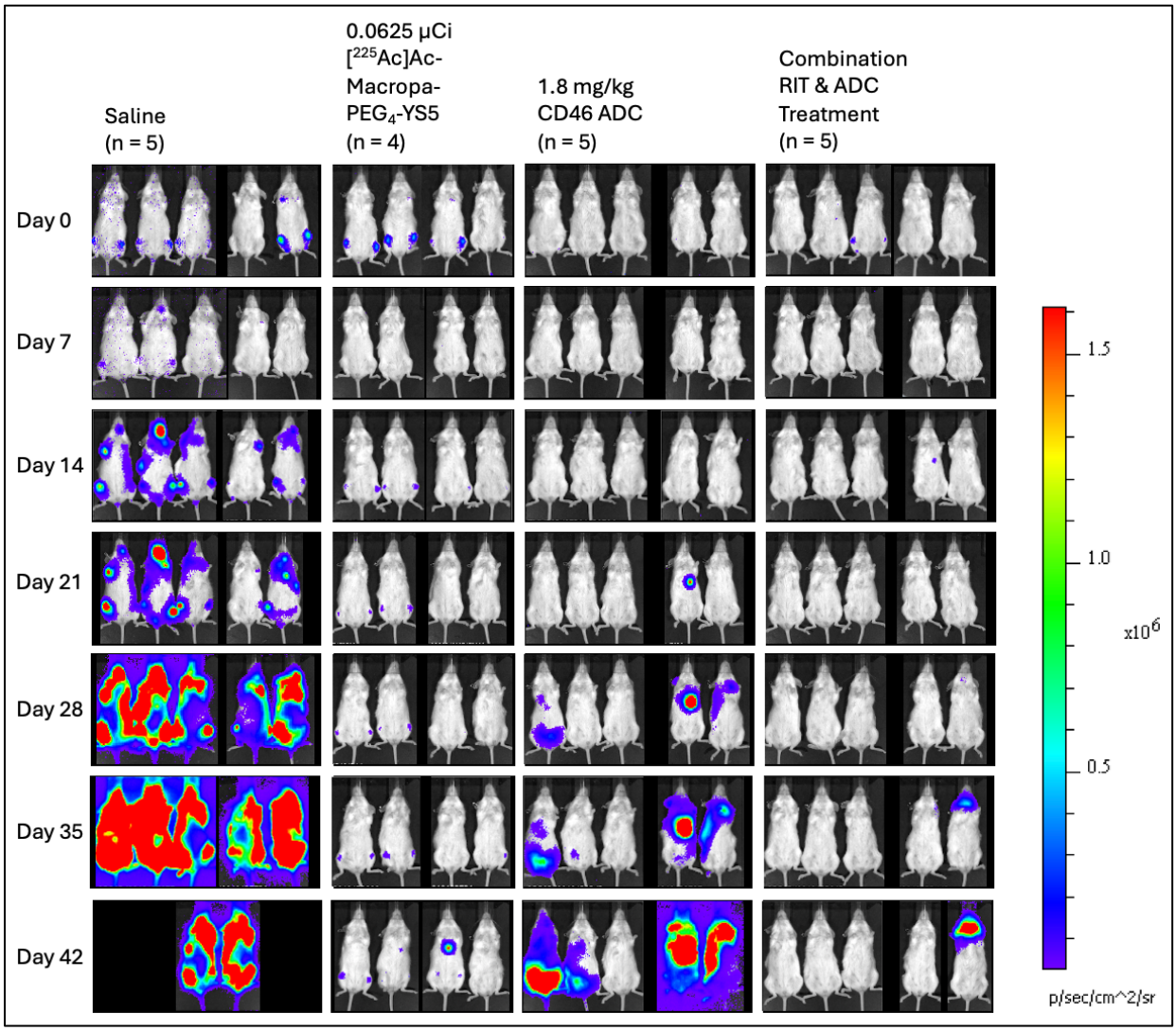

Figure 10: Bioluminescence imaging results for the RIT & ADC combination therapy pilot study through Day 42.

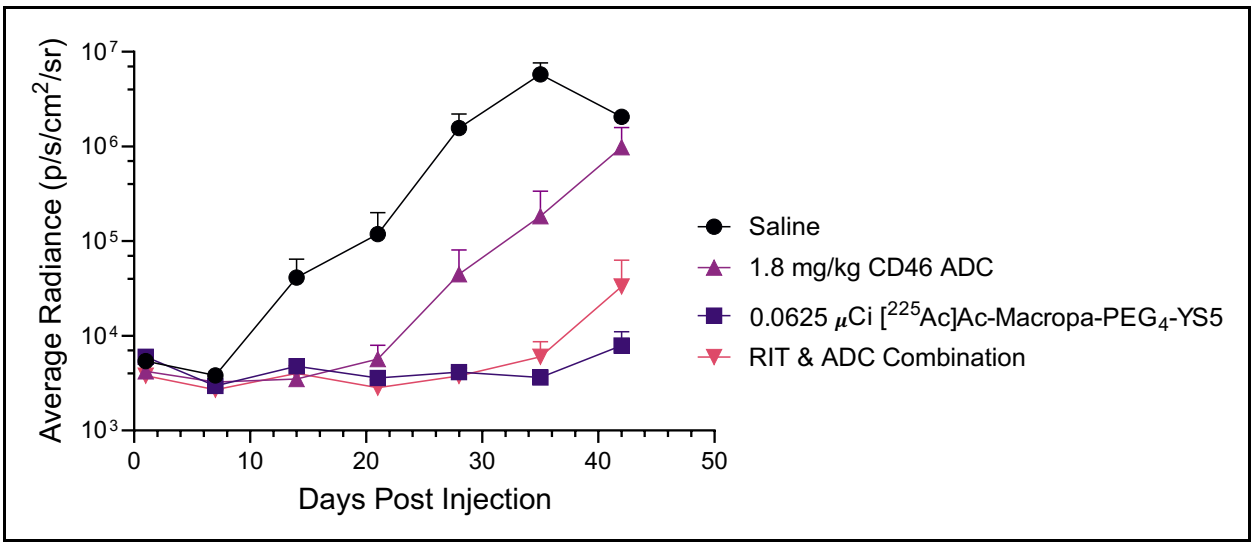

Figure 11: Results of average bioluminescent radiance, measured through Day 42. Average radiance was quantified in each mouse via whole body ROI and then averaged per experiment group.

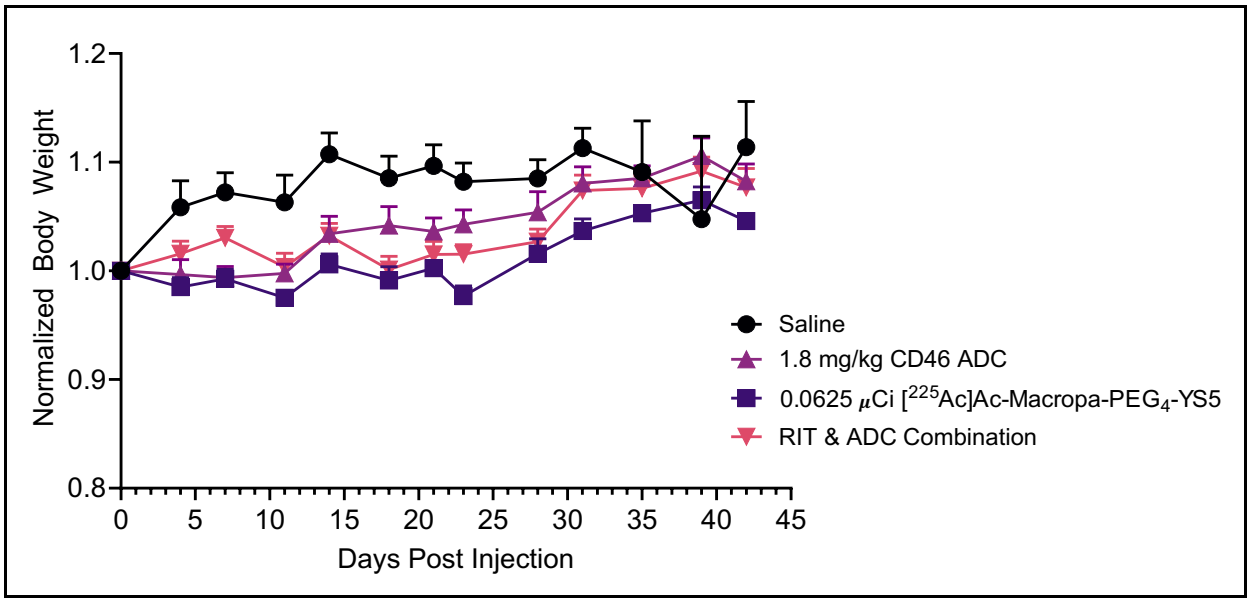

Figure 12: Body weight results for RIT & ADC combination therapy pilot study through Day 42. Results are normalized to the average body weight per experiment group measured at Day 0.

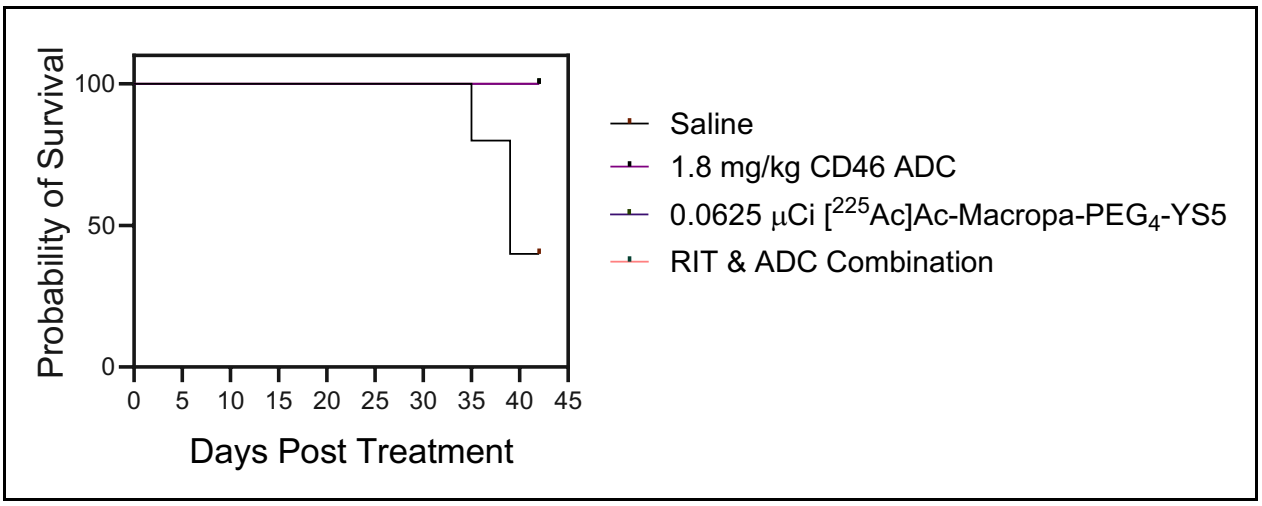

Figure 13: Kaplan-Meier plot displaying survival results per experiment group through Day 42. No treatment group mice died, while three saline mice were euthanized due to body weight loss and paralysis.

4 Discussion

Our group had several objectives in evaluating combination RIT & ADC therapy *in-vitro*. First, we aimed to reproduce the promising cell-killing efficacy results seen in previously reported CD46 ADC and [^{225}Ac]Ac-Macropa-PEG$_4$-YS5 monotherapy studies. Second, we hoped to gain insight into the mechanism of action of combination RIT & ADC treatment by assessing the interaction relationship between the two drugs. Finally, we wanted to report combination dosing levels that elicited high therapeutic efficacy to provide a reference for future work in this area.

The results of the monotherapy cell viability assays, seen in **Figures 7** and **8**, match well with prior literature. Our generated CD46 ADC IC$_{50}$ value of 0.37 nM closely resembles the 0.6 nM IC$_{50}$ value reported by Sherbenou, et al.[4] in their MM.1s cell viability study. [^{225}Ac]Ac-Macropa-PEG$_4$-YS5 had not previously been evaluated in a MM.1s cell viability assay, but the

recorded monotherapy IC_{50} value of 0.197 nCi/mL is similar to an IC_{50} value of 0.08 nCi/mL observed in a 22Rv1 prostate cancer cell line treated with [^{225}Ac]Ac-DOTA-YS5 by Bidkar, et al.[7]

For the combination RIT & ADC cell viability assay, drug concentrations centered around the monotherapy IC_{50} values were selected to best evaluate the cell-killing efficacy of combination therapy. The results of the dose-response matrix and ZIP plot in **Figure 9** indicate a strong overall therapeutic response of combination treatment, with evidence of enhanced potency of RIT & ADC treatment at some concentrations. This synergistic relationship suggests that multiple myeloma cells are more susceptible to damage and death when exposed to RIT & ADC therapies in tandem, with greater cell-killing possibly achieved at two lower combination doses than at a higher dose of monotherapy RIT or ADC.

Future *in-vitro* work will evaluate the efficacy of combination therapy in a colony formation assay, a study that measures the clonogenic growth ability of MM.1s cells following an initial treatment period. By measuring the combination concentrations that most successfully kill cells in the short term and stem cell proliferation in the long term, the drug interaction relationship between [^{225}Ac]Ac-Macropa-PEG$_4$-YS5 and CD46 ADC can be better understood and combination dosing can be further optimized for future experiments.

When designing the *in-vivo* combination therapy, our group aimed to achieve high antitumor efficacy of combination RIT & ADC treatment at doses that were *lower* than the best performing monotherapies in previously reported xenograft mouse models. The intention was to observe similar or superior therapeutic results to these prior studies while slowing the development of treatment resistance and minimizing off-target toxicities. The selected CD46 ADC dose of 1.8 mg/kg was less than half of the highest single dose tested in the xenograft study from Sherbenou, et al.[4] The chosen dose of 0.0625 μCi [^{225}Ac]Ac-Macropa-PEG$_4$-YS5 matched the lowest tested

single dose in the [^{225}Ac]Ac-DOTA-YS5 MM.1s xenograft study from Wadhwa, et al.[5] Furthermore, no fractionated dosing was examined in this pilot study.

Through the first 42 days of the study, all three treatment groups demonstrated antitumor efficacy compared to the saline group, highlighting the potency of both drugs even at low doses. Comparing results with the prior study from Wadhwa, et al.[5], the 0.0625 μCi [^{225}Ac]Ac-Macropa-PEG$_4$-YS5 monotherapy group at Day 42 appeared to feature less tumor burden than [^{225}Ac]Ac-DOTA-YS5 at Day 45, possibly indicating an efficacious benefit of the Macropa-PEG$_4$ conjugation compared to DOTA. While the ADC & RIT combination group featured only one mouse with noticeable tumor burden at Day 42, a definitive judgement on the efficacy of combination therapy compared to either monotherapy cannot be made. The increasing average body weights measured in all treatment groups is encouraging, providing early indication of an absence of significant disease symptoms or toxicity to non-target organs.

The *in-vivo* combination therapy remains ongoing. At study completion, blood and organ samples of surviving mice will be collected and analyzed for toxicity. Besides comparing this histological information to prior data from the [^{225}Ac]Ac-DOTA-YS5 monotherapy study by Wadhwa, et al.[5], this data can also be used to observe any possible toxicity due to CD46 ADC treatment. We also plan to image surviving mice with the aforementioned CD46-targeted tracer [^{89}Zr]Zr-DFO-YS5 or with [^{134}Ce]Ce-Macropa-PEG$_4$-YS5, a PET-imageable matched theranostic pair to [^{225}Ac]Ac-Macropa-PEG$_4$-YS5 that has recently been studied within the Flavell Lab. Either of these tracers can provide additional data on tumor burden within surviving mice, offering further comparison of the efficacy of treatment across groups. Since [^{134}Ce]Ce-Macropa-PEG$_4$-YS5 features the same Macropa chelator and PEG$_4$ linker as [^{225}Ac]Ac-Macropa-PEG$_4$-YS5, this tracer may also identify off-target areas subject to toxicity from RIT treatment.

There is significant opportunity for future work in this area. In both *in-vitro* and *in-vivo* components of this study, CD46 ADC and [^{225}Ac]Ac-Macropa-PEG$_4$-YS5 were given as treatments at the same time. It is feasible that staggered treatment regimens of the two drugs could result in better therapeutic efficacy. Another endeavor worthy of exploration is evaluating the treatment efficacy of CD46 ADC and [^{225}Ac]Ac-Macropa-PEG$_4$-YS5 conjugated to the *same* YS5 antibody, forming a single drug rather than two independent molecules. Finally, the *in-vivo* therapy in this work featured only single treatment doses of combination RIT & ADC therapy. A valuable next step is to compare these results to a combination therapy study that includes fractionated dosing regimens.

5 Conclusion

The recent development of the CD46-targeted therapies CD46 ADC and [^{225}Ac]Ac-Macropa-PEG$_4$-YS5 represent an exciting future for the treatment of multiple myeloma. In investigating the therapeutic efficacy of the two drugs used in combination across multiple preclinical models, this study provides valuable preliminary data that supports the further exploration of this treatment approach.

References

1. Siegel RL, Miller KD, Wagle NS, Jemal A (2023). Cancer statistics, 2023. *CA: A Cancer Journal for Clinicians*, *73*(1), 17-48
2. Rajkumar, S. V. (2022). Multiple myeloma: 2022 update on diagnosis, risk stratification, and management. *American Journal of Hematology*, *97*(8), 1086-1107.
3. Mol, I., Hu, Y., LeBlanc, T. W., Cappelleri, J. C., Chu, H., Nador, G., ... & Hlavacek, P. (2024). A matching-adjusted indirect comparison of the efficacy of elranatamab versus teclistamab in patients with triple-class exposed/refractory multiple myeloma. *Leukemia & Lymphoma*, *65*(5), 660-668.
4. Sherbenou, D. W., Aftab, B. T., Su, Y., Behrens, C. R., Wiita, A., Logan, A. C., ... & Liu, B. (2016). Antibody-drug conjugate targeting CD46 eliminates multiple myeloma cells. *The Journal of Clinical Investigation*, *126*(12), 4640-4653.
5. Wadhwa, A., Wang, S., Patiño-Escobar, B., Bidkar, A. P., Bobba, K. N., Chan, E., ... & Flavell, R. R. (2024). CD46-Targeted Theranostics for PET and 225Ac-Radiopharmaceutical Therapy of Multiple Myeloma. *Clinical Cancer Research*, *30*(5), 1009-1021.
6. Pandit-Taskar, N. (2019). Targeted radioimmunotherapy and theranostics with alpha emitters. *Journal of Medical Imaging and Radiation Sciences*, *50*(4), S41-S44.
7. Bidkar, A. P., Wang, S., Bobba, K. N., Chan, E., Bidlingmaier, S., Egusa, E. A., ... & Flavell, R. R. (2023). Treatment of prostate cancer with CD46-targeted 225Ac alpha particle radioimmunotherapy. *Clinical Cancer Research*, *29*(10), 1916-1928.

8. Wong, S., Imus, P., Mark, T., Kaufman, J., Imus, A., Zonder, J. A., ... & Martin, T. (2021). P-225: A first-in-human study of FOR46 in patients with triple refractory Multiple Myeloma. *Clinical Lymphoma Myeloma and Leukemia*, *21*, S164.
9. Bidkar A. (2023). Treatment of Prostate Cancer with CD46 Targeted ^{225}Ac Alpha Particle Radio-Immunotherapy – Beyond the Abstract. *UroToday*. https://www.urotoday.com/recent-abstracts/urologic-oncology/prostate-cancer/143663-treatment-of-prostate-cancer-with-cd46-targeted-225ac-alpha-particle-radioimmunotherapy-beyond-the-abstract.html. Accessed on August 29, 2024.
10. Abelman, R. O., Wu, B., Spring, L. M., Ellisen, L. W., & Bardia, A. (2023). Mechanisms of resistance to antibody–drug conjugates. *Cancers*, *15*(4), 1278.
11. Bobba, K. N., Bidkar, A. P., Wadhwa, A., Meher, N., Drona, S., Sorlin, A. M., ... & Flavell, R. R. (2024). Development of CD46 targeted alpha theranostics in prostate cancer using 134Ce/225Ac-Macropa-PEG4-YS5. *Theranostics*, *14*(4), 1344.
12. Sharma, S. K., Chow, A., Monette, S., Vivier, D., Pourat, J., Edwards, K. J., ... & Lewis, J. S. (2018). Fc-mediated anomalous biodistribution of therapeutic antibodies in immunodeficient mouse models. *Cancer Research*, *78*(7), 1820-1832.

Publishing Agreement

It is the policy of the University to encourage open access and broad distribution of all theses, dissertations, and manuscripts. The Graduate Division will facilitate the distribution of UCSF theses, dissertations, and manuscripts to the UCSF Library for open access and distribution. UCSF will make such theses, dissertations, and manuscripts accessible to the public and will take reasonable steps to preserve these works in perpetuity.

I hereby grant the non-exclusive, perpetual right to The Regents of the University of California to reproduce, publicly display, distribute, preserve, and publish copies of my thesis, dissertation, or manuscript in any form or media, now existing or later derived, including access online for teaching, research, and public service purposes.

Signed by:
Ellis Mayne
005398CE3A3347F...
Author Signature

8/29/2024
Date